FR9700747

I.P.N. - 91406 ORSAY CEDEX

institut de physique nucléaire CNRS - IN2P3 UNIVERSITÉ PARIS - SUD

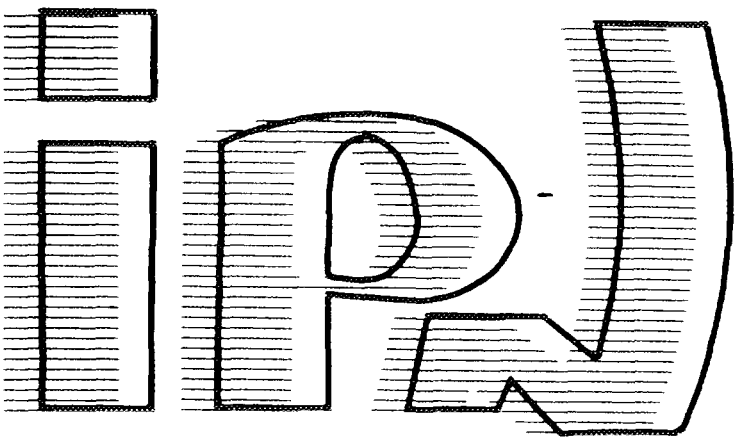

High spin structures in ^{184}Au

F. Ibrahim[1)], D. Hojman[2)], A.J. Kreiner[2)], B. Roussière[1)], J. Sauvage[1)], C. Bourgeois[1)], A. Korichi[1)], J. Davidson[2)], M. Davidson[2)], M. Debray[2)], I. Deloncle[3)], A. Knipper[4)], F. Le Blanc[1)], G. Marguier[5)], J. Oms[1)], N. Perrin[1)], M.G Porquet[3)], H. Sergolle[1)] et H. Somacal[2)].

1)Institut de Physique Nucléaire,91406 Orsay FRANCE
2)Departemento de Física, CNEA 1429 Buenos Aires, ARGENTINA
3)Centre de Spectrométrie Nucléaire et de Spectrométrie de Masse, Orsay FRANCE
4)Centre de Recherches Nucléaires, 67037 Strasbourg, FRANCE
5)Institut de Physique Nucléaire, 69621 Villeurbanne, FRANCE

IPNO DRE 95-09

à paraitre dans Phys. Rev. C

ROTATIONAL HIGH SPIN STRUCTURES IN DOUBLY-ODD ^{184}Au

F. Ibrahim[1], D. Hojman[2], A.J. Kreiner[2], B. Roussière[1], J. Sauvage[1],
C. Bourgeois[1], A. Korichi[1], J. Davidson[2], M. Davidson[2], M. Debray[2],
I. Deloncle[3], A. Knipper[4], F. Le Blanc[1], G. Marguier[5], J. Oms[1], N. Perrin[1],
M.G. Porquet[3], H. Sergolle[1], H. Somacal[2].

[1] Institut de Physique Nucléaire, 91406 Orsay Cedex, France.
[2] Departamento de Física, CNEA 1429 Buenos Aires, Argentina.
[3] Centre de Spectrométrie Nucléaire et de Spectrométrie de Masse,
91405 Orsay Cedex, France.
[4] Centre de Recherches Nucléaires, 67037 Strasbourg, France.
[5] Institut de Physique Nucléaire de Lyon , 69621 Villeurbanne, France.

Abstract : Excited states in the doubly-odd ^{184}Au nucleus have been studied by in-beam γ-ray spectroscopy. This nucleus was produced through the fusion-evaporation reactions ^{165}Ho(^{24}Mg, 5n), ^{170}Yb(^{19}F, 5n) and ^{161}Dy(^{27}Al, 4n). Different rotational band structures have been observed and interpreted as specific couplings of proton and neutron single-particle excitations present in neighboring odd Au and Pt nuclei.

PACS : 21.10.Re,21.60.Ev,27.70.+7

I. INTRODUCTION

Until recently[1,2] very little was known on the doubly-odd nucleus ^{184}Au[3,4]. A careful study[1,2] of the low-spin states of ^{184}Au populated in the β^+/EC decay of ^{184}Hg has recently been carried out establishing the spin and parity values of the ground state ($I^\pi=5^+$), the first excited long-lived isomer ($I^\pi=2^+$) and several other levels. Thus it provides a good basis onto which to construct other excitations. The ^{184}Au nucleus is on the upper edge of the prolate-deformed rare-earth region as documented by its odd-mass neighbors. The nuclei ^{183,185}Au show[5–7] band structure of prolate type (specifically πh9/2 and πi13/2 decoupled bands), while the shape coexistence is still present in both of them[8]. The situation changes for the isotones of ^{184}Au : ^{183}Pt[9,10] shows prolate structures only while ^{185}Hg[11,12] has states which are predominantly prolate, few others being oblate and less deformed. In recent years other doubly-odd nuclei of this mass-region have been studied : ^{182}Ir (the nearest doubly-odd isotone of ^{184}Au)[13–15], ^{184}Ir[16,17], ^{186}Ir[18,19] and ^{186}Au[20,21]. All our studies concerning doubly-odd nuclei occur in the frame of an effort to better understand the evolution of proton (p) and neutron (n) coupling schemes and to obtain information on p-n residual forces[14,16,22,23]. For this kind of work it is important to gather information on both high- and low-spin states in order to establish complete and reliable level schemes. The present investigation on ^{184}Au is the first one to be performed on yrast and near-yrast states. Preliminary results have been presented in Refs. 1), 2) and 24).

II. EXPERIMENTS

The first experiment was carried out at the TANDAR facility in Buenos Aires utilizing the ^{161}Dy(^{27}Al, 4n) reaction in order to establish the feasibility of populating excited states in ^{184}Au through the (H.I., xn) fusion evaporation process. An excitation function was measured but as the yield was found to be small, two other experiments were performed at the Orsay Tandem accelerator. The first experiment utilized the ^{165}Ho(^{24}Mg, 5n) reaction with a 1mg/cm^2 Ho target supported by a 0.1 mm Th backing in order to stop the recoiling nuclei. Emitted γ-rays were detected by the "Château de Cristal" array[25] comprising 10 Compton suppressed large volume Ge detectors, two planar Ge detectors and an inner

ball of 26 BaF_2 scintillators for multiplicity and total energy determination. An excitation function was measured in the 120-135 MeV bombarding energy range in 5 MeV steps. In this energy range the production of ^{184}Au was optimum at 135 MeV which was the highest reachable energy beam at the Tandem. Since the beam intensity was not large enough at that energy the experiment was performed at 130 MeV. We have thus recorded 2.2×10^7 events with the requirement that at least two Ge detectors and two BaF_2 counters fired in 100 ns time interval.
The second experiment was performed using the ^{170}Yb(^{19}F, 5n) reaction (1 mg/cm^2 ^{170}Yb target on a 0.2 mm Pb backing) and an excitation function was measured between 95 and 110 MeV (5 MeV steps). The maximum yield for this reaction takes place at 105 MeV where the production of ^{185}Au is still high. The γ-γ coincidence experiment was hence done at 107 MeV using 11 HP Ge counters of the array. We have thus recorded 1.6×10^8 events with the requirement that at least two Ge detectors and one BaF_2 counter fired in 100 ns time interval. In both data sets the intensity of individual transitions in ^{185}Au corresponding to the 4n channel is significant in comparison with those of ^{184}Au where the population is probably much more fragmented. Moreover fission of the Au compound nuclei makes up for an important fraction of the total γ-γ intensity. For example in fig. 1, which shows a gate on the 269.8 keV line, one can clearly see transitions known to belong to the fission fragment ^{106}Ru. Another important pollutant in these experiments is ^{184}Pt[26] directly produced by proton evaporation and radioactive decay. Fortunately the level schemes of ^{185}Au and ^{184}Pt are well known from previous studies[6,7,26]. Coincidences relationships with Au K_α X-rays permitted, after identification of ^{185}Au lines, an unambiguous assignment of lines to ^{184}Au. Figures 2, 3 and 4 show spectra gated on some of the strongest transitions in ^{184}Au. Extensive gating allowed the construction of four different band structures in this nucleus.

III. BAND STRUCTURE

Fig. 5 displays the four band structures identified in ^{184}Au. No detailed connection to the known low-spin part of the level scheme could be established while band b) and c) show clear evidence of coincidences with the 156.4 keV line, most likely the strongest transition observed in the decay work and which deexcites the

69±6 ns isomer[1,2]. This half-life could explain why the 156.4 keV is attenuated in the coincident spectra. Furthermore, members of bands a) and c) are in coincidence with each other (see Fig. 4) but the linking path ways could not be determined. On the other hand band d) stands alone with no connections to the other bands, nor to previously known states.

It is worth noting that band a) is the one with the strongest population, which indicates that it is very likely built on the ground state or on a state very close to it.

Since no firm spin and parity assignments can be made in the present work, our discussion is therefore based on systematics and theoretical arguments. Most of the structures formed in doubly-odd nuclei of this mass-region have very characteristic features which make their identification almost unique and which have led to a general classification scheme[22,23,27]. In order to set the frame for the discussion let us first identify the single n and p quasiparticle states present in the neighboring nuclei and from them build the zero-order level sequence for ^{184}Au. This information is given in Fig. 6. Prolate and oblate states are given respectively on the left and right-hand lower side. Oblate νi13/2, νp3/2 and πd3/2 excitations are taken from ^{185}Hg and ^{185}Au respectively since they are not known in ^{183}Pt and ^{183}Au where, if existing, they are located at higher energies. In the doubly-odd nucleus the levels involving these oblate states are very likely also located at higher energies.

From the point of view of the zero-order scheme the situation looks very much like the one in ^{182}Ir[13] where the $\nu 1/2^-[521]\otimes\pi$h9/2 doubly-decoupled band (DDB)[22] provides the ground-state structure, followed in excitation energy by the $\nu 7/2^-[514]\otimes\pi$h9/2 compressed band[16,27] and the semidecoupled[16,27] $\nu 9/2^+[624]\otimes\pi$h9/2 structure. We already know that the ground state of ^{186}Au corresponds to a prolate shape[20] and that the prolate part of the high-spin excitation spectrum lies at the lowest energy so that one expects a similar situation in ^{184}Au.

However in comparing the zero-order levels shown in Fig. 6 and the level scheme established in the decay work[1,2] one notes an inversion of the configurations. Indeed, the 5^+ ground-state corresponds, very likely, to the $\nu 7/2^-[514]\otimes\pi$h9/2 structure while the DDB may be associated with the $I^\pi=2^+$ isomer at 68.6 keV. This inversion which does not take place in the lighter isotone ^{182}Ir[13–15] is not

completely clarified but may be related to a deformation change effect[14,28,29]. Nevertheless the following discussion on the band structure is largely independent of the radioactivity results since it relies on the characteristic features of the bands themselves. A cranking analysis has been performed in order to extract inertia parameters and alignments which are given in Table I. The values fit into the systematics and one obtains a reasonable additivity for the alignments.

The DDB candidate presented in Fig. 5 band d) is compared in Fig. 7 with the ground-state bands of ^{182,184}Pt along with the DDB in ^{182}Ir and its Z-1 even-even Os neighbors. It resembles very much the DDB in ^{182}Ir and the other ones in the mass-region[22]. Most likely the sequence is based on a 5^+ state, but one expects[22] a 3^+ state a few keV below taking into account that the lowest state of h9/2 parentage both in ^{183,185}Au is the $5/2^-$ one[19]. Calculations have been performed in the framework of the rotor-plus-two-quasiparticle coupling model as described in Refs. 30) and 31) for the isotones ^{182}Ir and ^{184}Au. For the $\nu 1/2^-[521]\otimes\pi$h9/2 structure in ^{182}Ir the 3^+ state is predicted to be the lowest lying level with a 5^+ state a few keV above it. The 2^+ and 4^+ states of this structure are predicted at higher energies and very close to the 3^+ and 5^+ states respectively. On the other hand for the same structure in ^{184}Au, the 2^+ and 4^+ states are situated below the 3^+ and 5^+ levels respectively. In the latter case one would expect an unfavored band more populated that the one recently observed in ^{182}Ir[15].

The band b) shown in Fig. 5 exhibits a feature which is characteristic of a structure called semidecoupled[13,16], namely a staggering of the M1 transition energies, and has been studied in several doubly-odd nuclei of this region[13]. It consists here of the coupling of an aligned h9/2 proton (which thus participates only with its favored signature) and a high-K i13/2 neutron. The perturbation (staggering) present in the rotational band of the doubly-odd nucleus just reflects the perturbation in the νi13/2 bands of neighboring odd-mass nuclei. Here it is most likely that the neutron Fermi level lies nearest to the $9/2^+[624]$ orbit. Fig. 8 shows a comparison between the νi13/2 and the semidecoupled bands for the isotones ^{181}Os, ^{182}Ir, ^{183}Pt, ^{184}Au and ^{185}Hg. The striking resemblance between the structures provides the basis for the spin assignments suggested for ^{184}Au. Fig. 9 shows a more detailed comparison between ^{182}Ir and ^{184}Au and also for the pair of isotones ^{184}Ir and ^{186}Au. It is apparent that the staggering is more pronounced for the N=105 isotones on account of the lower position of the neutron Fermi surface

within the νi13/2 multiplet. The semidecoupled structure usually starts with a set of low energy M1 transitions which are rather strongly converted and therefore easy to miss if the low-energy sensitivity of the experiment is not particularly good. The additivity of the alignments is also satisfactory here (see Table I), namely i_{np}^{exp}=5.41$\hbar$ vs. i_{np}^{calc}=i_n(νi13/2 ^{183}Pt)+i_p(πh9/2 ^{183}Au)=2.99+2.97=5.96$\hbar$.

The band a) shown in Fig. 5 is the one with the strongest feeding and is therefore the best candidate for the yrast band. The most natural assumption is that this band is built on the 5^+ ground state or on a relatively high-spin nearby lying state and most likely related to the $\nu 7/2^-[514]\otimes\pi$h9/2 structure. A structure of this parentage is known in ^{182}Ir[13] to be built on a 5^+ state but it starts with much smaller transition energies (39, 75, 107...keV). In fig. 10 one can see the $\nu 7/2^-[514]$ and $\nu 7/2^-[514]\otimes\pi$h9/2 structures in the isotonic chain ^{181}Os, ^{182}Ir, ^{183}Pt, ^{184}Au and ^{185}Hg. A more detailed comparison between ^{182}Ir and ^{184}Au is shown in Fig. 11. The lowest state of the ^{184}Au cascade has been assigned as 6^+, based purely on similarity of transition energies. In fact a rotor-plus-two-quasiparticle calculation performed using the approaches described in Refs. 30), 31) and 32), yields for the lowest states of this structure two close lying levels namely $I^\pi=5^+$ and 6^+. These states are rather K-admixed, showing significant ($\nu 7/2\pm\pi 1/2$) K=4, 3 and ($\nu 7/2+\pi 3/2$) K=5 components. From a theoretical point of view such a structure does not show a rigid rotor behaviour corresponding to a given K value but displays a kind of distortion called compression[16,27]. On the other hand the observed band shows an unexpected extremely rigid behaviour which corresponds here to K=4, as can be obtained from the energy ratio of the first two M1 transitions. The reason for this feature is not understood in the framework of the suggested interpretation.

Finally the band c) shown on Fig. 5 will be briefly discussed. This band also displays a staggering which is somewhat less pronounced than in band b). The only way to produce this distortion is to couple a "staggered" excitation (the νi13/2 in this region of the periodic table) to a completely decoupled structure. The πh9/2 has already been employed but in both ^{183,185}Au another decoupled excitation is known, namely πi13/2. In fact a structure similar to ours has been interpreted[21] as νi13/2$\otimes\pi$i13/2 in ^{186}Au. A higher-statistics experiment[33] has modified the results given in Ref. 21) leaving the structure as shown in Fig. 12. This recent measurement has in particular not confirmed the linking transitions

to the νi13/2$\otimes\pi$h9/2 structure[21].

Furthermore the fact that the staggering is more pronounced in ^{184}Au than in ^{186}Au is consistent with the lower position of the neutron Fermi level in the νi13/2 multiplet resembling the behavior for the semidecoupled structure (νi13/2$\otimes\pi$h9/2), observed in the other isotopic series, for instance Ir, Re[13].

Another feature of this structure which is also consistent with the proposed assignment is the fact that the ΔI=1, M1 transitions are much stronger than in the other structures. Indeed, we can see on figure 2 and 3 that M1 transitions have much weaker intensities than E2 transitions. On the other hand, on figure 4, 145.2, 151.4, 180.7, 209.7 keV M1 transitions and 360, 390.8, 439.7, 488.9 keV E2 transitions have similar intensities. This is basically due to the fact[16] that the i13/2 proton has an expectation value of the third component of the intrinsic spin, $<s_3>>0$ (contrary to πh9/2), and that[34] the πi13/2 alignment is larger than that of the πh9/2 (see Table I).

IV. CONCLUSIONS

The nucleus ^{184}Au has been studied for the first time through in-beam γ-ray spectroscopy techniques following (H.I., xn) fusion-evaporation reactions. Four rotational bands have been established, discussed in term of proton and neutron excitations present in the neighboring odd-mass nuclei, and interpreted on the basis of the existing classification for structures in deformed doubly-odd nuclei. Several questions are still open, notably the nature of the very rigid ΔI=1 (K=4) cascade, the confirmation of the νi13/2$\otimes\pi$i13/2 assignment to one of the structures and the relative location of the bands. An experiment using a new-generation 4π array is needed.

References

1) F. Ibrahim thèse, Université Paris VII, 1994.

2) F. Ibrahim et al., Z. Phys A350,9(1994) and ref. therein.

3) R. Eder et al., Hyp. Int. 60,83(1990).

4) W.G. Nettles et al., J. Phys.39,343(1978).

5) M.P. Carpenter, thesis and Prog. Rep. Nucl. Spec. (1988)26.

6) M.G. Desthuilliers et al., Nucl. Phys. A313,221(1979).
7) A.J. Larabee et al., Phys. Lett. 169B,21(1986).
8) M.I. Macias-Marques et al., Nucl. Phys. A427,205(1984).
9) B. Roussière et al., Nucl. Phys. A504,511(1989).
10) J. Nyberg et al., Nucl. Phys. A511,92(1990).
11) P. Dabkiewicz et al., Phys. Lett. 82B,199(1979).
12) F. Hannachi et al., Z. Phys. A330,15(1988).
13) A.J. Kreiner et al., Phys. Rev. C42,878(1990).
14) J. Sauvage et al., Nucl. Phys. to be published.
15) H. Somacal et al., to be published.
16) A.J. Kreiner et al., Nucl. Phys. A489,525(1988).
17) A. Ben Braham et al., Nucl. Phys. A482,553(1988).
18) A.J. Kreiner et al., Nucl. Phys. A432,451(1985).
19) A. Ben Braham et al., Nucl. Phys. A533,113(1991).
20) M.G. Porquet et al., Nucl. Phys. A411,65(1983).
21) V.P. Janzen et al., Phys. Rev. C45,613(1992).
22) A.J. Kreiner "Exotic Nuclear Spectroscopy", Plenum Press 1990(Ed. W.Mc Harris) and references therein.
23) A.J. Kreiner, "Nuclear Shapes and Nuclear Structure at Low excitation Energies", Plenum Press, Serie B : Physics Vol. 289 143(1992)(Eds. J.Sauvage, M. Vergnes).
24) F. Ibrahim et al., INFFS6 Bernkastel Kues 1992, Inst. Phys. Conf. Ser. $N^0$132 (1993) 731.
25) F.A. Beck, Conf. on Instrumentation for Heavy-Ions Nuclear Research (Oak Ridge,1984) Ed D. Schapira (New York : Harwood Academic) p129.
26) M.P. Carpenter et al., Nucl. Phys. A513,125(1990).
27) A.J. Kreiner, "Contemporary Topics in Nuclear Structure" World Scientific 1988 (Eds. R.F. Casten, A. Frank, M. Moshinsky and S. Pittel), p. 521-540.
28) F. Ibrahim et al., proc. of E.N.A.M 1995 (Arles) to be published.
29) F. Ibrahim et al., in preparation.
30) L. Bennour et al., Nucl. Phys. A465,35(1987).
31) L. Bennour, thèse Université Paris XI.
32) A.J. Kreiner, Z. Phys., A288,373(1978).
33) M.G. Porquet, private communication.

34) F. Dönau and S. Frauendorf, Proc. Conf. on High Angular Momentum Properties of Nuclei (Oak Ridge, 1982) Ed N.R. Johson (New York : Harwood Academic) p. 143.

FIGURE CAPTIONS

Fig. 1 - Spectrum in coincidence with the 269.8 keV γ-ray. The open square indicates contamination from fission fragment (^{106}Ru). Lines labeled with a) and c) correspond to the structures a) and c) of fig. 5. Energies are given in keV.

Fig. 2 - Spectra in coincidence with lines in ^{184}Au. Lines labeled with a), b) and c) correspond to the structures a), b) and c) of fig. 5. Energies are given in keV.

Fig. 3 - Spectra in coincidence with lines in ^{184}Au. Lines labeled with black squares and a), b), c) correspond respectively to ^{184}Pt and to the structures a), b) and c) of fig. 5. Energies are given in keV.

Fig. 4 - Sum of the spectra in coincidences with the 151.4, 180.7, 209, 278.9, 517.5 and 560.3 keV lines of ^{184}Au. Lines labeled with black dot, open triangle and open square correspond respectively to the structures a), b) and c) of fig. 5.

Fig. 5 - The four bands observed in ^{184}Au with their tentative assignments.

Fig. 6 - Single quasiparticle states present in the four odd-mass neighboring nuclei of ^{184}Au (upper part). The cross indicates states corresponding to a prolate nuclear shape and the open dot states with an oblate nuclear shape. Zero-order level scheme for ^{184}Au (lower part). Prolate and oblate states are given respectively on the left and right-hand side.

Fig. 7 - Comparison of ground-state bands in the even-even nuclei ^{182,184}Pt and ^{180,182}Os[25] with the doubly-decoupled band in ^{182}Ir[13-15)] and band d) in ^{184}Au.

Fig. 8 - Comparison of νi13/2 bands in the odd-mass isotones ^{181}Os, ^{183}Pt and ^{185}Hg[26)] with the νi13/2$\otimes\pi$h9/2 semidecoupled band in ^{182}Ir[13-15)] and band b) in ^{184}Au.

Fig. 9 - Comparison of the νi13/2$\otimes\pi$h9/2 semidecoupled structures in the pairs of isotones ^{182}Ir, ^{184}Au (band b)) and ^{184}Ir, ^{186}Au.

Fig. 10 - Comparison of $\nu 7/2^-[514]$ bands in the isotones ^{181}Os, ^{183}Pt and ^{185}Hg with the $\nu 7/2^-[514]\otimes\pi$h9/2 band in ^{182}Ir and the candidate (band a)) in ^{184}Au.

Fig. 11 - Detailed comparison of the $\nu 7/2^-[514]\otimes\pi$h9/2 structure in ^{182}Ir[13–15] with band a) in ^{184}Au.

Fig. 12 - Comparison of the proposed[21,32] νi13/2$\otimes\pi$i13/2 structure in ^{186}Au along with band c) in ^{184}Au.

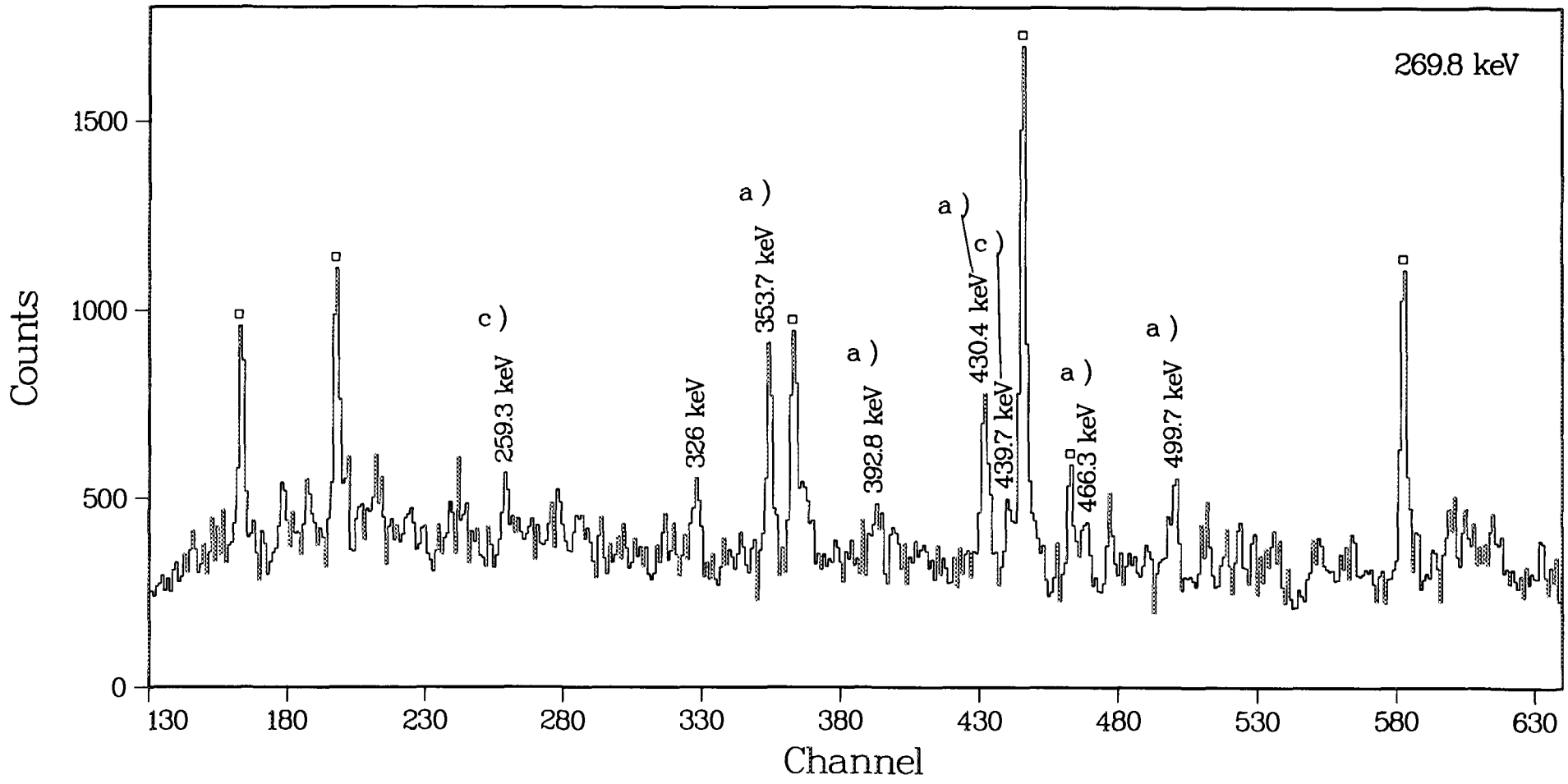
269.8 keV
1500
1000
500
0
Counts
c)
259.3 keV
326 keV
a)
353.7 keV
a)
392.8 keV
a)
430.4 keV
c)
439.7 keV
a)
466.3 keV
a)
499.7 keV
130
180
230
280
330
380
430
480
530
580
630
Channel

Fig. 1

Fig 2.

Counts
Channel
353.7 keV
269.8
430.4
499.7
563.0
533.5+533.9 keV
156.4
197.3 b)
227.3 a)
312.0 a)
321.4 b)
392.8 a)
440.3 b)
466.3 a)
312.0 keV
103.5 a)
124.0 a)
180.7 c)
209.5 c)
227.3 a)
390.8 c)
392.8 a)
439.7 c)
466.3 a)
495
517.5 c)
533.5 a)
550

Fig. 3

Counts
611.6 keV
156.4
269.8 a)
321.4 b)
366
387.8 b)
440.3 b)
533.9 b)
Counts
476.9 keV
156.4
263.7 b)
321.4 b)
387.8 b)
550 b)
Counts
156.4 keV
263.7 b)
321.4 b)
387.8 b)
440.3 b)
476.9 b)
517.5 c)
533.9 b)
Channel

gate 151+181+209+280+518+560 keV
Counts
Channel
0
1000
2000
3000
50
100
150
200
250
300
350
400
450
500
550
600
650
103.5 keV
124.0 keV
145.2 keV
151.4 keV
156.4 keV
180.7 keV
209.5 keV
227.3 keV
259.3 keV
269.8 keV
278.9 keV
296 keV
312.0 keV
353.7 keV
360 keV
390.8 keV
439.7 keV
468.5 keV
488.9 keV
517.5 keV
560.3 keV

fig. 4

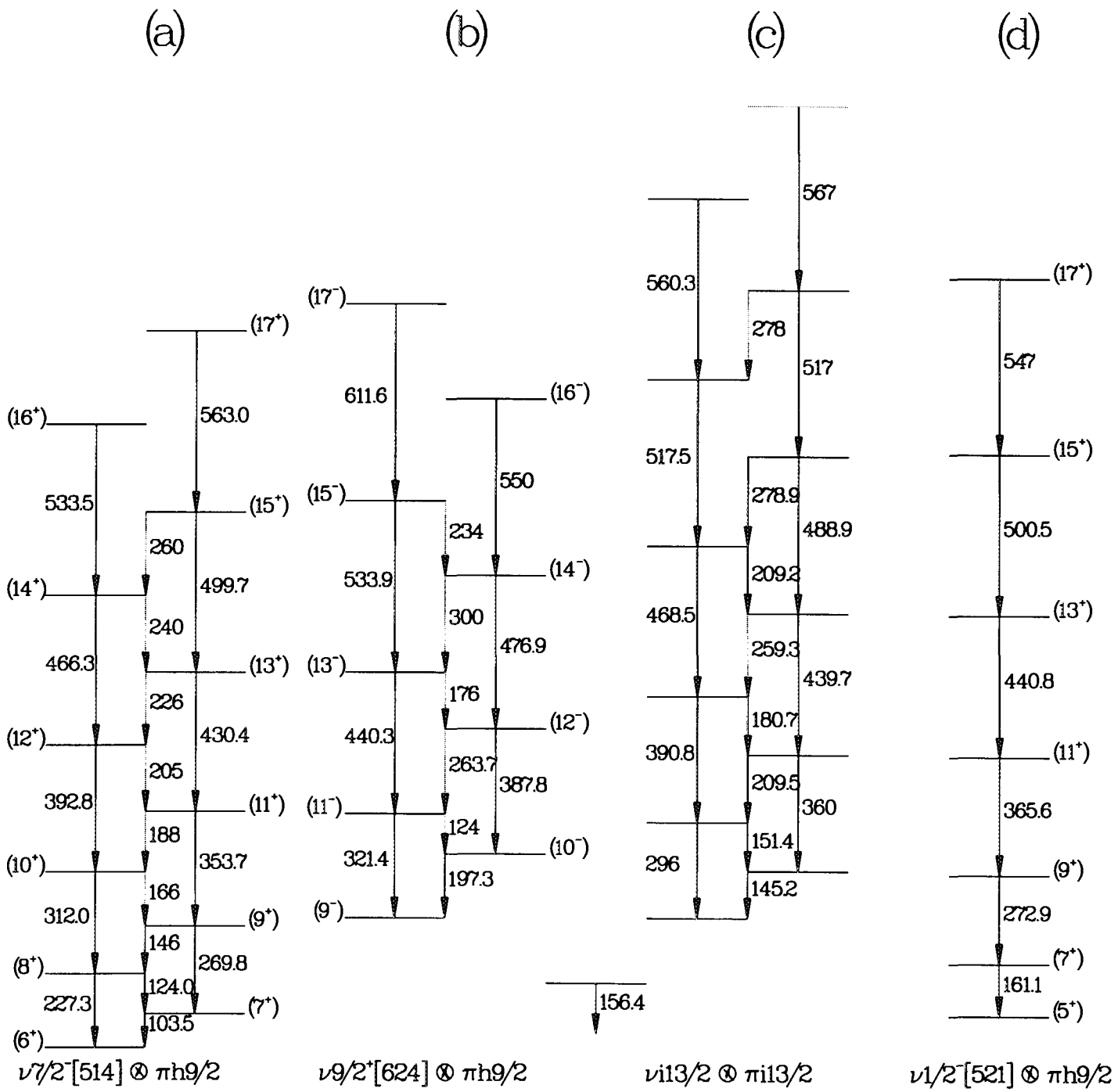
(a)
(b)
(c)
(d)
(17+)
(16+)
563.0
533.5
(15+)
260
(14+)
499.7
240
466.3
(13+)
226
(12+)
430.4
205
392.8
(11+)
188
(10+)
353.7
166
312.0
(9+)
146
(8+)
269.8
124.0
227.3
(7+)
103.5
(6+)
ν7/2-[514] ⊗ πh9/2
(17-)
611.6
(16-)
550
(15-)
234
(14-)
533.9
300
476.9
(13-)
176
(12-)
440.3
263.7
387.8
(11-)
124
(10-)
321.4
197.3
(9-)
156.4
ν9/2+[624] ⊗ πh9/2
567
560.3
278
517
517.5
278.9
488.9
209.2
468.5
259.3
439.7
180.7
390.8
209.5
360
151.4
296
145.2
νi13/2 ⊗ πi13/2
(17+)
547
(15+)
500.5
(13+)
440.8
(11+)
365.6
(9+)
272.9
(7+)
161.1
(5+)
ν1/2-[521] ⊗ πh9/2

Fig. 5

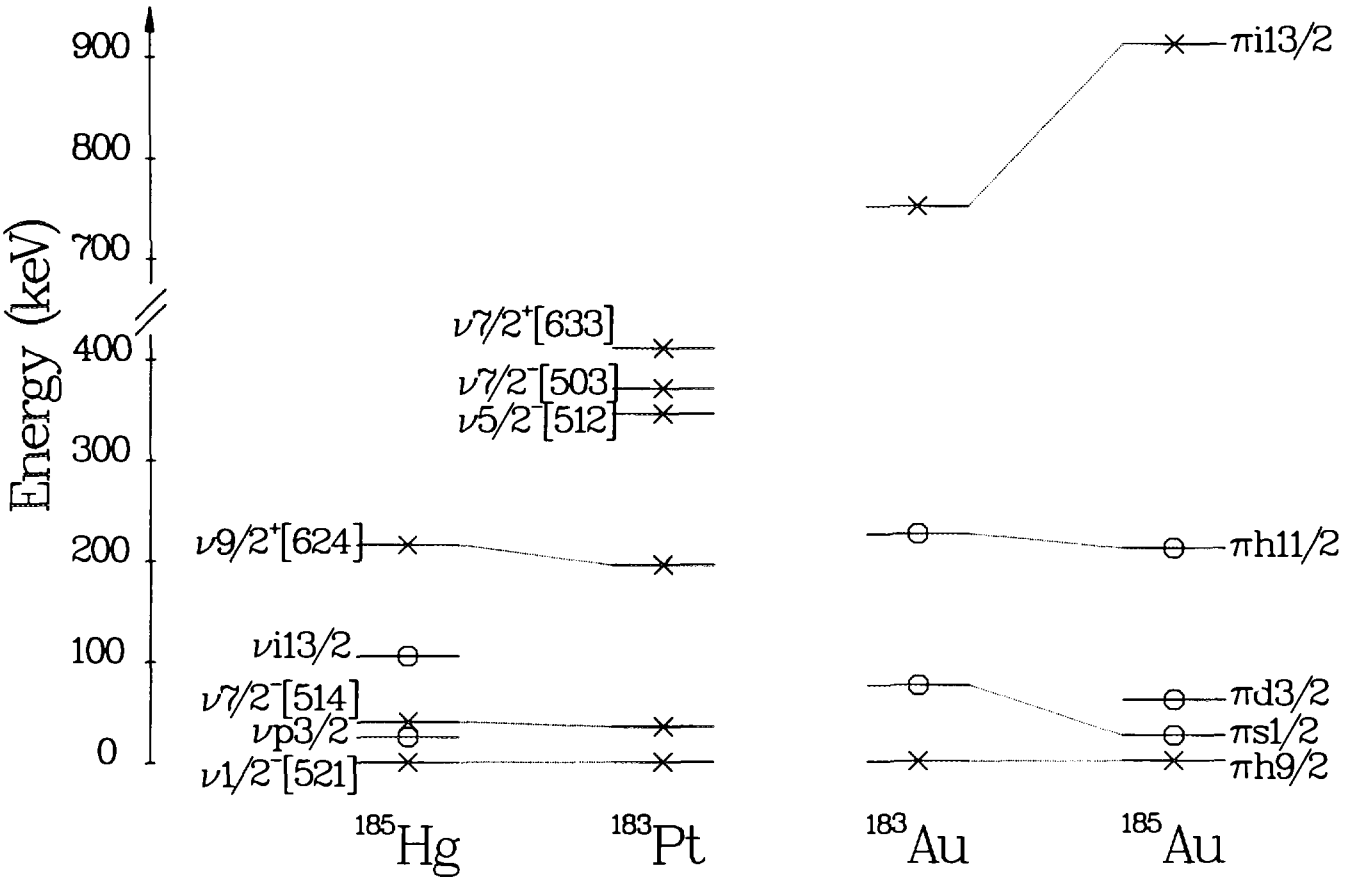
Energy (keV)
900
800
700
400
300
200
100
0
ν7/2⁺[633]
ν7/2⁻[503]
ν5/2⁻[512]
ν9/2⁺[624]
νi13/2
ν7/2⁻[514]
νp3/2
ν1/2⁻[521]
πi13/2
πh11/2
πd3/2
πs1/2
πh9/2
185Hg
183Pt
183Au
185Au

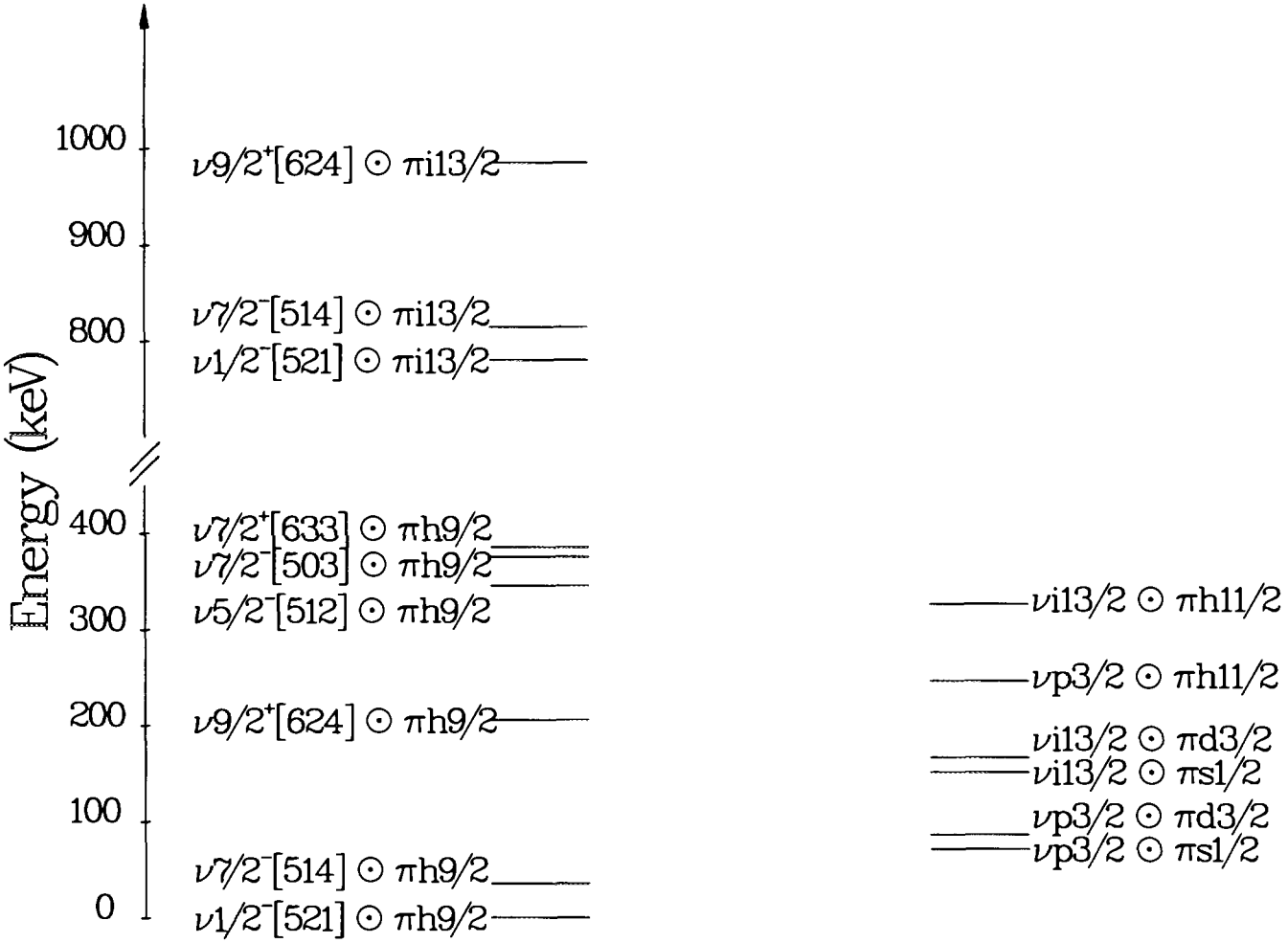
Energy (keV)
1000
900
800
400
300
200
100
0
ν9/2⁺[624] ⊙ πi13/2
ν7/2⁻[514] ⊙ πi13/2
ν1/2⁻[521] ⊙ πi13/2
ν7/2⁺[633] ⊙ πh9/2
ν7/2⁻[503] ⊙ πh9/2
ν5/2⁻[512] ⊙ πh9/2
ν9/2⁺[624] ⊙ πh9/2
ν7/2⁻[514] ⊙ πh9/2
ν1/2⁻[521] ⊙ πh9/2
νi13/2 ⊙ πh11/2
νp3/2 ⊙ πh11/2
νi13/2 ⊙ πd3/2
νi13/2 ⊙ πs1/2
νp3/2 ⊙ πd3/2
νp3/2 ⊙ πs1/2

fig. 6

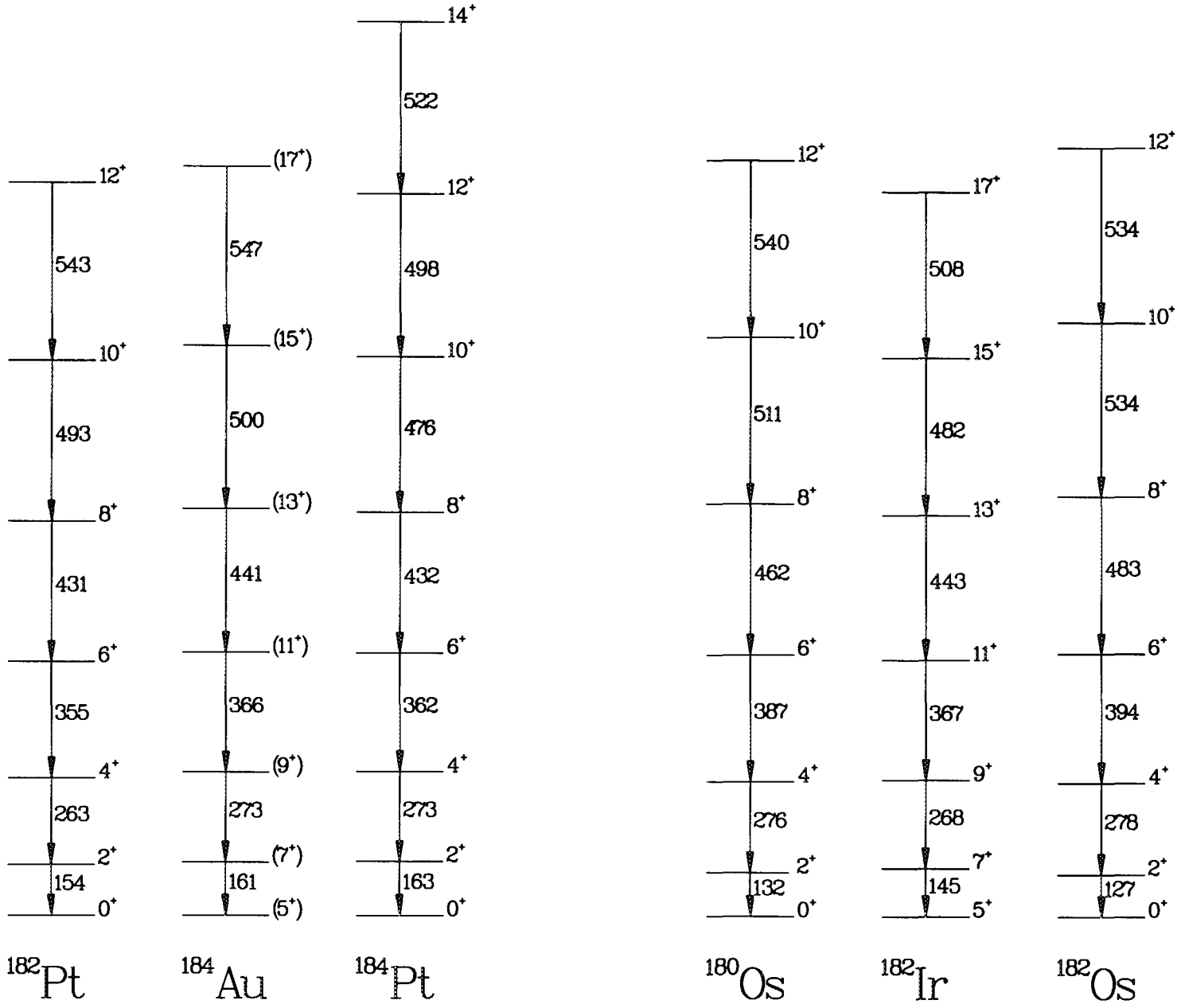
12+
543
10+
493
8+
431
6+
355
4+
263
2+
154
0+
182Pt
(17+)
547
(15+)
500
(13+)
441
(11+)
366
(9+)
273
(7+)
161
(5+)
184Au
14+
522
12+
498
10+
476
8+
432
6+
362
4+
273
2+
163
0+
184Pt
12+
540
10+
511
8+
462
6+
387
4+
276
2+
132
0+
180Os
17+
508
15+
482
13+
443
11+
367
9+
268
7+
145
5+
182Ir
12+
534
10+
534
8+
483
6+
394
4+
278
2+
127
0+
182Os

fig. 7

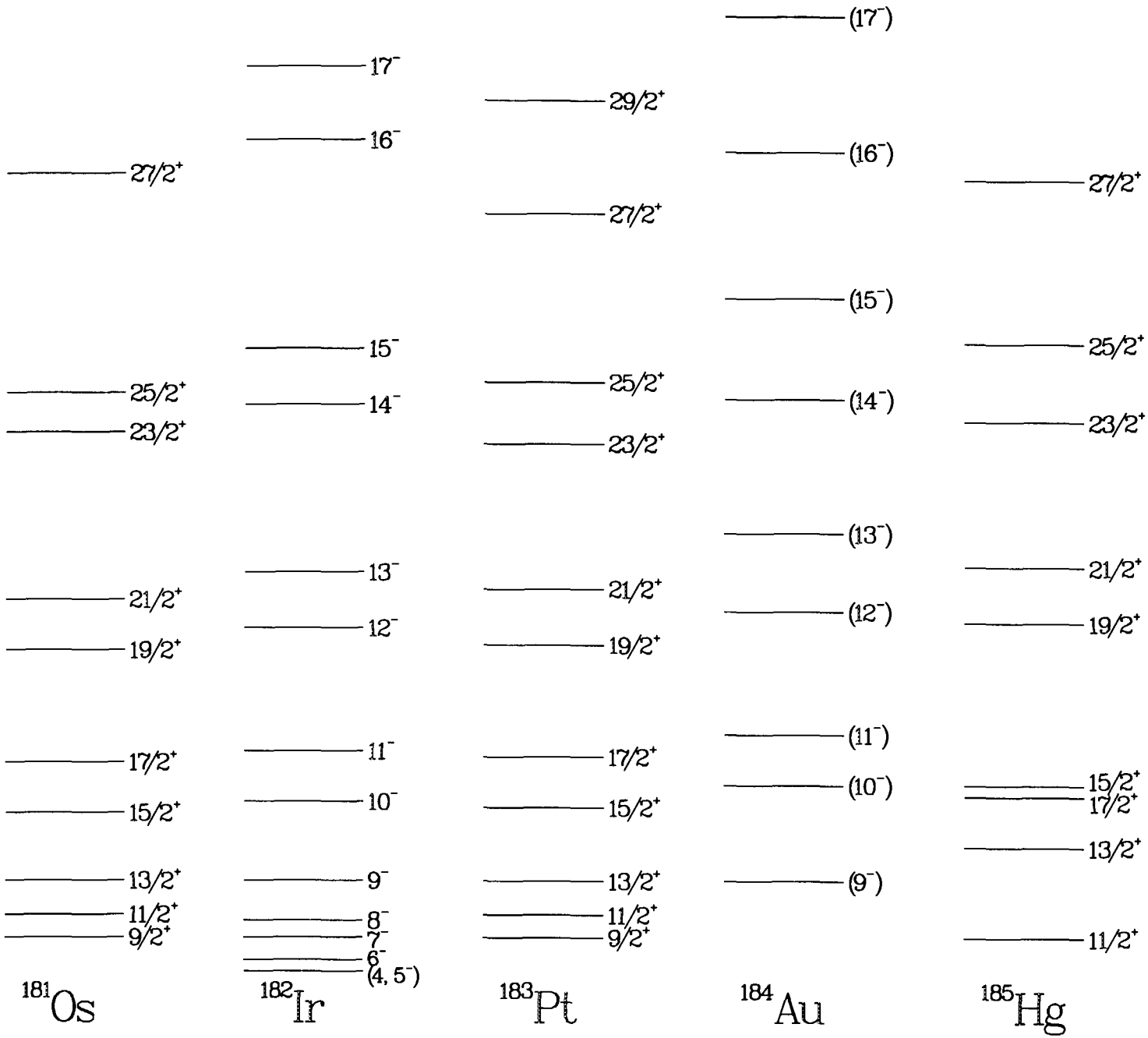
27/2+
25/2+
23/2+
21/2+
19/2+
17/2+
15/2+
13/2+
11/2+
9/2+
181Os
17−
16−
15−
14−
13−
12−
11−
10−
9−
8−
7−
6−
(4, 5−)
182Ir
29/2+
27/2+
25/2+
23/2+
21/2+
19/2+
17/2+
15/2+
13/2+
11/2+
9/2+
183Pt
(17−)
(16−)
(15−)
(14−)
(13−)
(12−)
(11−)
(10−)
(9−)
184Au
27/2+
25/2+
23/2+
21/2+
19/2+
15/2+
17/2+
13/2+
11/2+
185Hg

fig. 8

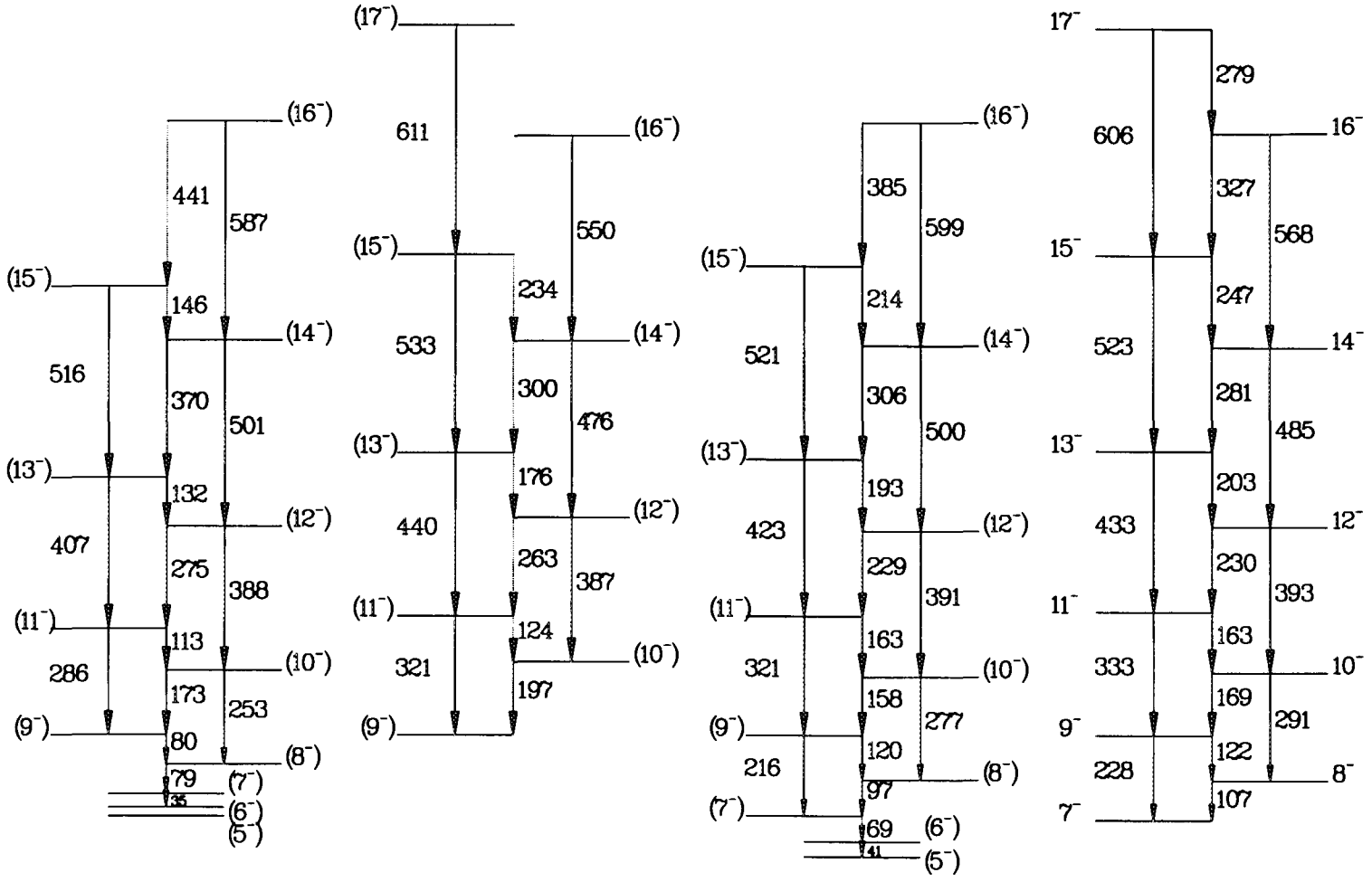

^{182}Ir ^{184}Au ^{184}Ir ^{186}Au

fig. 3

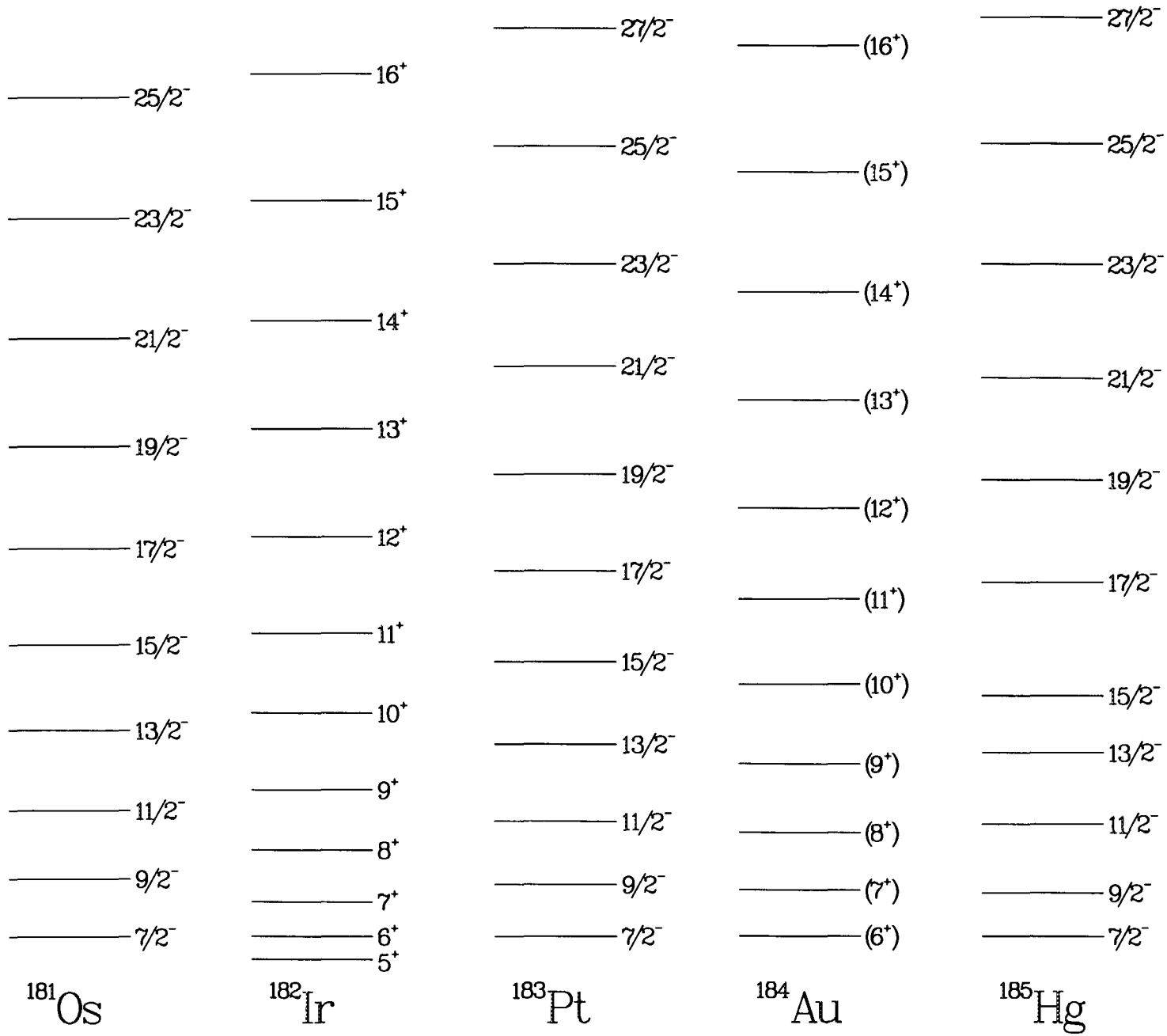
25/2⁻
23/2⁻
21/2⁻
19/2⁻
17/2⁻
15/2⁻
13/2⁻
11/2⁻
9/2⁻
7/2⁻
181Os
16⁺
15⁺
14⁺
13⁺
12⁺
11⁺
10⁺
9⁺
8⁺
7⁺
6⁺
5⁺
182Ir
27/2⁻
25/2⁻
23/2⁻
21/2⁻
19/2⁻
17/2⁻
15/2⁻
13/2⁻
11/2⁻
9/2⁻
7/2⁻
183Pt
(16⁺)
(15⁺)
(14⁺)
(13⁺)
(12⁺)
(11⁺)
(10⁺)
(9⁺)
(8⁺)
(7⁺)
(6⁺)
184Au
27/2⁻
25/2⁻
23/2⁻
21/2⁻
19/2⁻
17/2⁻
15/2⁻
13/2⁻
11/2⁻
9/2⁻
7/2⁻
185Hg

fig. 10

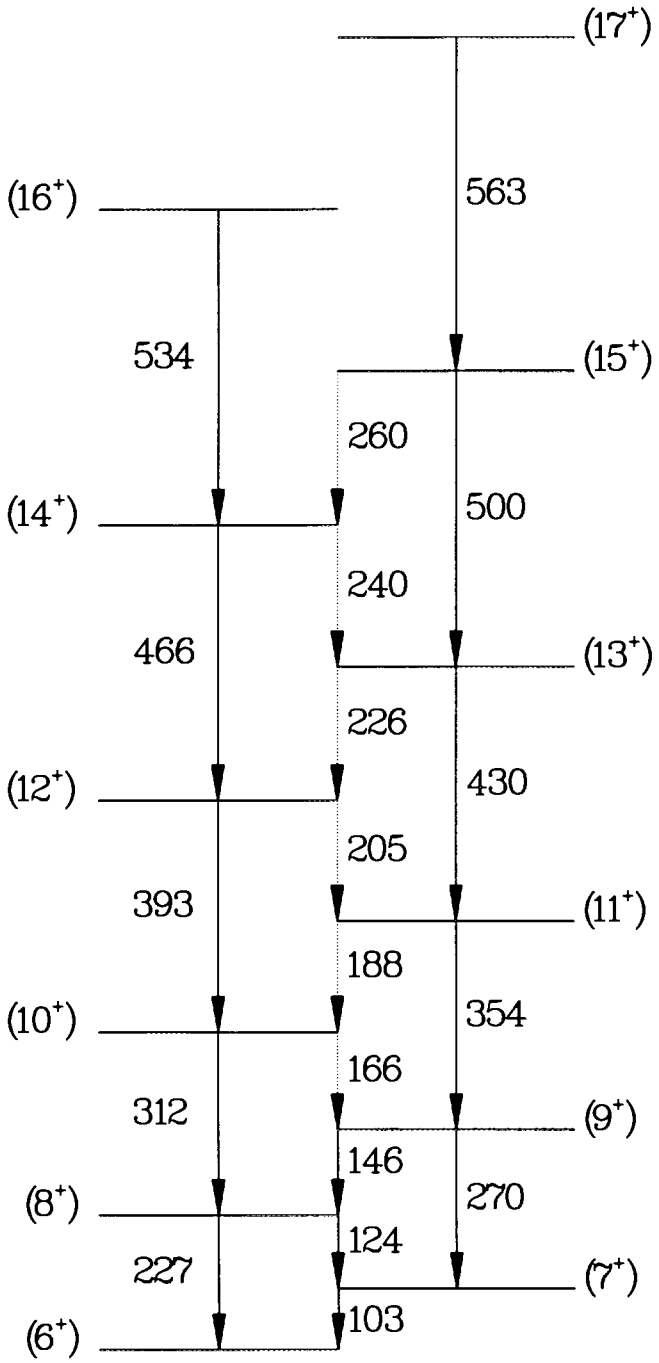

^{184}Au

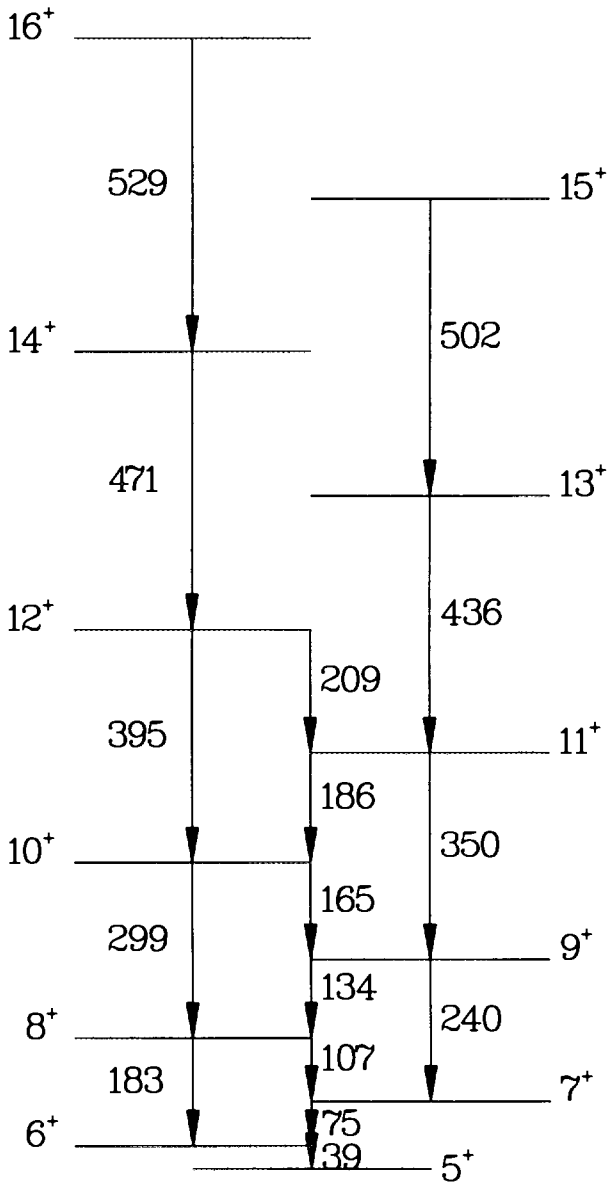

^{182}Ir

fig. 11

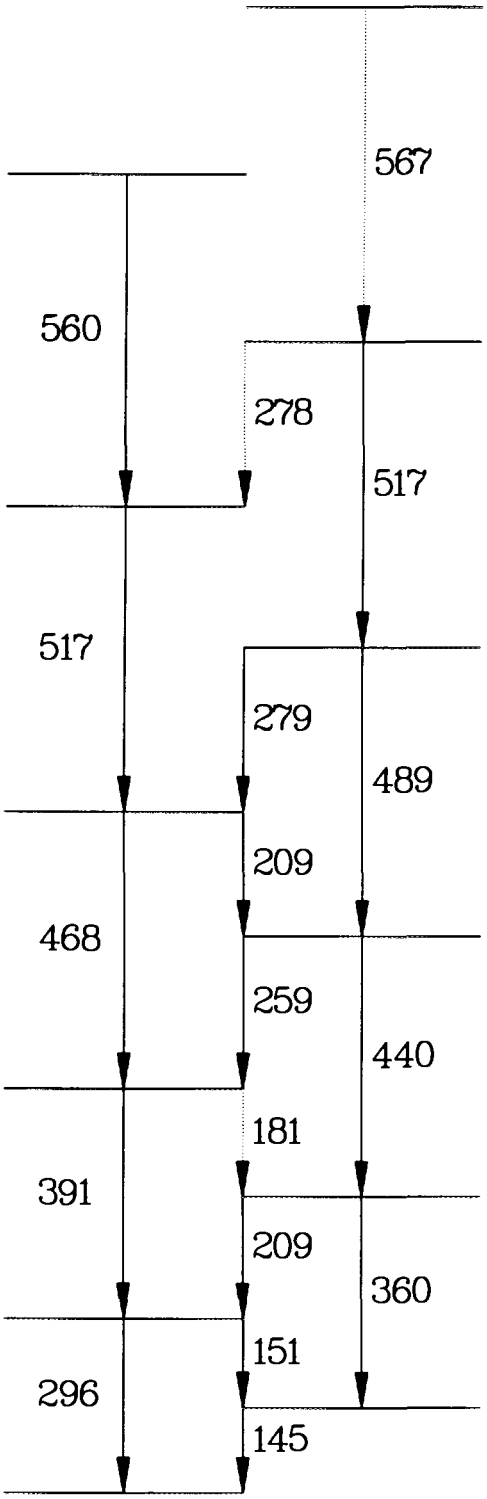

^{184}Au

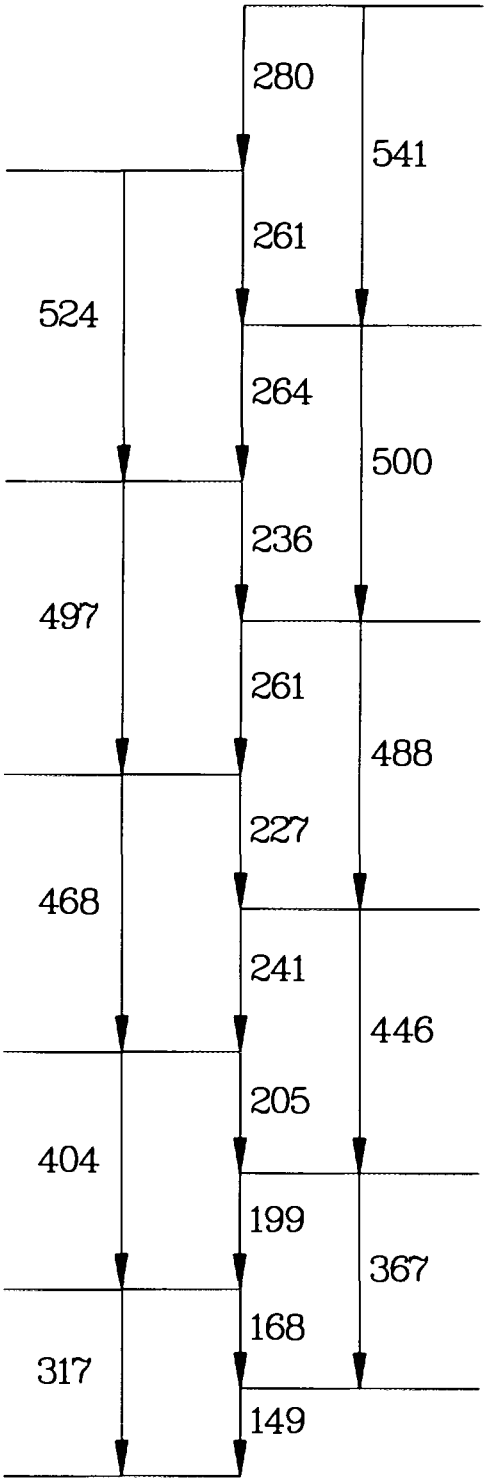

^{186}Au

fig. 12.